JOURNAL OF GEOPHYSICAL RESEARCH, VOL. 111, D12311, doi:10.1029/2005JD006758, 2006

Closing the global radiocarbon budget 1945–2005

Tobias Naegler[1,2] and Ingeborg Levin[1]

Received 18 October 2005; revised 18 January 2006; accepted 1 March 2006; published 23 June 2006.

[1] The global radiocarbon cycle of the last 60 years was simulated with the Global Radiocarbon Exploration Model (GRACE). The total radiocarbon production by atmospheric nuclear bomb tests was determined using available stratospheric and tropospheric radiocarbon (^{14}C) observations as constraints. To estimate the range of uncertainty in the explosive force of atmospheric nuclear bomb tests and their respective ^{14}C yield factor, we applied different published bomb test compilations. Furthermore, to account for a possible small bias in the available stratospheric excess radiocarbon observations, we tested the different bomb test compilations with both uncorrected and corrected stratospheric ^{14}C observations. For each of these scenarios of the total bomb ^{14}C burden, the model simulated the distribution of excess radiocarbon among the stratosphere, troposphere, biosphere, and ocean carbon reservoirs. With a global bomb ^{14}C production of $598–632 \cdot 10^{26}$ atoms (99–105 kmol) ^{14}C between 1945 and 1980, simulated excess radiocarbon inventories are in good agreement with all available stratospheric and tropospheric radiocarbon observations as well as with the latest estimates of the ocean excess radiocarbon inventories during the GEOSECS and WOCE surveys from Peacock (2004) and Key et al. (2004). For the very first time, our model is thus capable of closing the excess radiocarbon budget on the basis of our current knowledge of exchange rates and reservoir sizes in the global carbon system.

Citation: Naegler, T., and I. Levin (2006), Closing the global radiocarbon budget 1945–2005, *J. Geophys. Res.*, *111*, D12311, doi:10.1029/2005JD006758.

1. Introduction

[2] Human activity has affected the natural balance of radiocarbon in the Earth system since the beginning of the industrial revolution. Owing to the relatively short half life of radiocarbon of 5730 years, fossil carbon is free of radiocarbon. Thus the extensive release of fossil fuel-derived CO_2 into the atmosphere causes an ongoing decrease of the atmospheric ^{14}C-to-C ratio (Suess-Effect), unbalancing the preindustrial isotopic equilibrium between the atmosphere, the ocean, and the biosphere, and in consequence, leading to a net flux of radiocarbon from the ocean and the biosphere to the atmosphere over the last century. However, today the Suess-Effect is superimposed by an even larger disturbance, namely the effects of the production of so-called bomb radiocarbon in atmospheric nuclear weapon tests between 1945 and 1980 (peaking in 1961/1962). Bomb radiocarbon was formed when thermal neutrons originating from the bomb tests reacted with atmospheric nitrogen to form radiocarbon. Injected mainly into the stratosphere, bomb radiocarbon is oxidized to $^{14}CO_2$ and, like natural radiocarbon, takes part in the global carbon cycle. Observed radiocarbon inventory changes in the carbon reservoirs since prebomb times therefore always reflect the production of radiocarbon in nuclear bomb tests (and a much smaller contribution by the nuclear industry) as well as the redistribution of radiocarbon due to the Suess-Effect. Throughout this study, we will refer to radiocarbon inventory changes since the onset of atmospheric nuclear bomb tests in 1945 as "excess radiocarbon." (Note that many previous studies referred to "bomb radiocarbon" when "excess radiocarbon" would have been more adequate).

[3] Excess radiocarbon is widely established as a tracer in environmental studies. In particular, it is used to study dynamics within and exchange processes among the main carbon reservoirs: the stratosphere, the troposphere, the biosphere, and the ocean [*Levin and Hesshaimer*, 2000]. Still, the quantitative budget of excess radiocarbon, i.e., the total amount of bomb radiocarbon produced in atmospheric nuclear bomb tests, its subsequent distribution among the carbon reservoirs, and the redistribution of radiocarbon among the carbon reservoirs due to the Suess-Effect, remained uncertain. Closing the excess radiocarbon budget, however, is of particular scientific interest because a model simulation of the excess radiocarbon inventories in good agreement with available observations in all carbon reservoirs is an excellent and widely accepted test of global carbon cycle models and their parameterizations of carbon exchange processes among the relevant reservoirs: Accurate determination of ^{14}C inventories can provide important constraints, for example on atmospheric transport [*Johnston et al.*, 1976; *Kjellström et al.*, 2000; *Land et al.*, 2002;

[1]Institut für Umweltphysik (IUP), Heidelberg, Germany.
[2]Also at Laboratoire des Sciences du Climat et de l'Environnement (LSCE), Gif-sur-Yvette, France.

0148-0227/06/2005JD006758$09.00

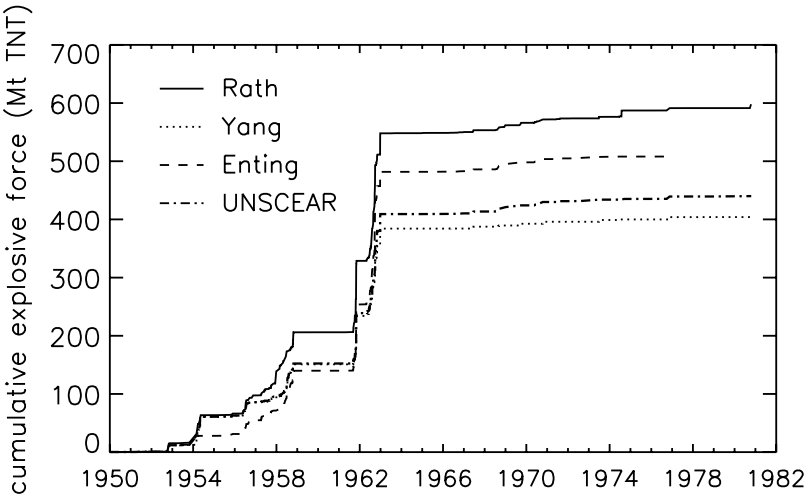

Figure 1. Cumulative explosive force of atmospheric nuclear bomb tests (in Mt TNT) for the bomb test compilations from *Enting* [1982], *Rath* [1988], *UNSCEAR* [2000], and *Yang et al.* [2000]. Total explosive forces until 1980 are 512 Mt TNT for the compilation from Enting, 598 Mt TNT for the compilation from Rath, 440 Mt TNT for UNSCEAR, and 405 Mt TNT for Yang et al.

Naegler, 2005] and on air-sea gas exchange of CO_2 [*Broecker et al.*, 1985; *Wanninkhof*, 1992]. On the other hand (and of similar importance), a successful simulation of the excess radiocarbon inventories also serves as a consistency check of observation-based inventory estimates, which are often difficult to obtain.

[4] A number of difficulties complicate the quantitative assessment of the global excess ^{14}C budget: On the production side, the amount of bomb ^{14}C released by atmospheric nuclear weapon tests is difficult to estimate. *Glasstone and Dolan* [1977] assume that almost every neutron released in a nuclear bomb test, after being slowed down to "thermal" energy levels, finally reacts with atmospheric nitrogen to produce radiocarbon. However, although several different compilations of atmospheric nuclear bomb tests are available [*Enting*, 1982; *Rath*, 1988; *U.N. Science Committee on the Effects of Atomic Radiation* (*UNSCEAR*), 2000; *Yang et al.*, 2000] which list the date, the location, and the explosive force (which is usually given in equivalents of megatons (Mt) of TNT) of the tests, no compilation of neutron production rates has been published. To complicate matters, the neutron (and thus the radiocarbon) production rates also depend on the type of nuclear bomb [*Glasstone and Dolan*, 1977]. However, lacking exact information on the production rates, as a first approximation, the bomb radiocarbon production is generally assumed to be proportional to the explosive force of atmospheric nuclear bomb tests.

[5] Most estimates of the global bomb radiocarbon production relied on a single, constant radiocarbon yield factor (i.e., the number of ^{14}C atoms produced per Mt TNT) which is meant to represent the average radiocarbon yield per Mt TNT over all bomb tests (see also discussion in section 2.2). However, owing to the large differences in total number and the explosive force of atmospheric nuclear bomb tests as listed in the different bomb test compilations (see Figure 1), it is indispensable to calibrate the bomb radiocarbon yield factor individually for each bomb test compilation with the help of a carbon cycle model constrained with global (excess) radiocarbon observations. Table 1 summarizes respective attempts by *Enting and Pearman* [1982], *Hesshaimer et al.* [1994], and *Lassey et al.* [1996]. (Note: To quantify the bomb radiocarbon production and the excess radiocarbon inventories in the different carbon cycle compartments, respectively, we use the SI-unit 1 kmol = $6.022 \cdot 10^{26}$ atoms in parallel with the "classical" unit 10^{26} atoms ^{14}C throughout the text. This convention facilitates the comparison of our results with those from previous studies, which are often given in multiples of 10^{26} atoms ^{14}C.)

Table 1. Previous Estimates of the Bomb Radiocarbon Yield Factor and Total Bomb Radiocarbon Production[a]

		Yield Factor ^{14}C Production/Mt TNT		Total ^{14}C Production		
Publication	Bomb Test Compilation	10^{26} Atoms	kmol	10^{26} Atoms	kmol	Data Constraints
Enting and Pearman [1982]	*Enting* [1982]	1.776	0.295	909	151.0	T[1]
Hesshaimer et al. [1994]	*Rath* [1988]	1.050	0.174	628	104.3	T[2] & S[3]
Lassey et al. [1996]	*Enting* [1982]	1.352	0.225	631	104.8	S[4]
Lassey et al. [1996]	*Rath* [1988]	1.144	0.185	684	113.6	S[4]

[a]Previous estimates of the radiocarbon yield factor (in 10^{26} atoms, kmol ^{14}C per Mt TNT, respectively) and the total cumulative bomb radiocarbon production (in 10^{26} atoms, kmol ^{14}C, respectively). In the last column, T and S indicate that the radiocarbon yield factor was constrained by tropospheric and/or stratospheric radiocarbon observations, respectively. The references for the atmospheric data constraints are the following: [1]*Nydal et al.* [1980], *Tans* [1981], [2]*Levin et al.* [1985], *Manning et al.* [1990], *Nydal and Lövseth* [1996], [3]*Telegadas* [1971], [4]"Available stratospheric data, ca. 1955–1969" (probably from *Telegadas* [1971]).

Table 2. Overview of Previous Estimates of the Ocean Excess Radiocarbon Inventory[a]

	GEOSECS (1975)		WOCE (1995)	
Publication	10^{26} Atoms	kmol	10^{26} Atoms	kmol
Broecker et al. [1980]	314 ± 30	52.2 ± 5.0		
Broecker et al. [1985]	289	48.0		
Lassey et al. [1990]	303	50.3		
Broecker and Peng [1994]	350[b]	58.1[b]		
Broecker et al. [1995]	305 ± 30	50.7 ± 5.0		
Jain et al. [1997]	327 ± 33	54.3 ± 5.5		
Sweeney et al. [2004]	215 ± 5	35.7 ± 0.8	328 ± 13	54.5 ± 2.2
Peacock [2004][c]	241 ± 60	40.0 ± 10.0	335 ± 15	55.6 ± 2.5
Corrected by *Naegler et al.* [2006][d]	245 ± 60	40.7 ± 10.0	340 ± 15	56.5 ± 2.5
Peacock [2004][e]	262 ± 26	43.5 ± 4.3		
Corrected by *Naegler et al.* [2006][c]	264 ± 26	43.9 ± 4.3		
Key et al. [2004]			315 ± 47	52.3 ± 7.8
Corrected by *Naegler et al.* [2006][c]			355 ± 50	59.0 ± 8.3

[a]Overview of previous estimates of the ocean excess radiocarbon inventory based on oceanographic data from the time of the GEOSECS (1975) and WOCE (1995) surveys.
[b]Corrected to "$\sim 3.0 \cdot 10^{28}$ atoms" (=49.8 kmol ^{14}C) in the same paper.
[c]Multitracer correlation approach.
[d]Negligence of some ocean regions in the approaches of *Peacock* [2004] and *Key et al.* [2004] leads to an underestimation of the global ocean excess radiocarbon inventory. *Naegler et al.* [2006] corrected the inventories for this negligence.
[e]Corrected silicate approach, similar to *Broecker et al.* [1995].

[6] Not only the production of bomb radiocarbon is difficult to quantify but also data-based estimates of excess radiocarbon inventories in the main carbon reservoirs are challenging. Tropospheric excess radiocarbon inventories can be calculated from available high-precision long-term records of tropospheric Δ^{14}C [*Levin et al.*, 1985, 1987, 1999; *Manning et al.*, 1990; *Nydal and Lövseth*, 1996; *Levin and Kromer*, 2004] (see also overview in the work of *Naegler* [2005]). However, stratospheric, oceanic, and biospheric inventories are more difficult to assess due to difficulties in separating the natural radiocarbon component from the measured total ^{14}C and/or due to generally low sampling densities in space and time.

[7] For the stratosphere a large number of radiocarbon observations between 1955 and 1971 have been published in the reports of the Health and Safety Laboratories (HASL) (see overview in the work of *Telegadas* [1971]). However, the quality of these data has long been debated [*Tans*, 1981; *Broecker and Peng*, 1994] until *Hesshaimer and Levin* [2000] and *Naegler* [2005] could show that the HASL data set is of high quality and possible biases due to sample contamination or calibration difficulties are small. *Telegadas* [1971] first estimated stratospheric excess radiocarbon inventories from the HASL data. Finally, *Hesshaimer and Levin* [2000] and *Naegler* [2005] developed a more objective approach to calculate quarterly respective monthly mean excess radiocarbon inventories for subdivisions of the stratosphere from the HASL data, including a correction for increasing atmospheric CO_2 and decreasing atmospheric δ^{13}C. These corrected stratospheric HASL data are used in this study (see below).

[8] Numerous methods have been developed to estimate the oceanic excess radiocarbon inventory based on oceanographic data, either by tracer correlation methods [*Broecker et al.*, 1980, 1985; *Lassey et al.*, 1990; *Broecker and Peng*, 1994; *Broecker et al.*, 1995; *Peacock*, 2004; *Key et al.*, 2004] or by inverse ocean modeling [*Sweeney et al.*, 2004] (see Table 2 for a summary). These estimates range from 35.7 to 57.3 kmol ^{14}C ($215-345 \cdot 10^{26}$ atoms ^{14}C) for the time of the GEOSECS ocean survey (Geochemical Ocean Sections Study, 1972–1979, usually reported with respect to the reference year 1975) and 52.3 to 59.0 kmol ^{14}C ($315-355 \cdot 10^{26}$ atoms ^{14}C) for the time of the WOCE survey (World Ocean Circulation Experiment, 1990–2002, reference year 1995). The estimates from *Peacock* [2004] (multitracer correlation approach) and *Key et al.* [2004] are based on the most complete data sets and on the most reliable methods to separate the natural component from the excess (bomb and Suess-Effect) component. However, the data sets employed by both *Peacock* [2004] and *Key et al.* [2004] did not cover the full ocean. *Naegler et al.* [2006] estimated the amount of missing excess radiocarbon due to this lack in spatial coverage with an Ocean General Circulation Model (OGCM). Furthermore, the WOCE radiocarbon data for the North Atlantic were sampled mainly in the late 1980s, almost a decade earlier than the WOCE reference year of 1995. *Naegler et al.* [2006] therefore corrected the *Key et al.* [2004] inventory estimate for this temporal bias. The corrected ocean excess radiocarbon inventory estimates from *Naegler et al.* [2006] are also quoted in Table 2.

[9] In contrast to the other main carbon reservoirs, no attempt has been made to estimate the total excess radiocarbon inventory of the global terrestrial biosphere based on observations. Owing to the large spatial and structural inhomogeneity of the terrestrial biosphere, available Δ^{14}C measurements do not provide data representative for the large-scale radiocarbon distribution in this reservoir.

[10] A number of studies tried to reconcile (simple) carbon cycle models with available excess radiocarbon data [*Enting and Pearman*, 1982; *Hesshaimer et al.*, 1994; *Broecker and Peng*, 1994; *Lassey et al.*, 1996; *Jain et al.*, 1997]. Most of these studies found a serious mismatch between model and observations, blaming either the stratospheric ^{14}C observations from the HASL reports [*Broecker and Peng*, 1994] or the ocean excess radiocarbon inventory estimates from *Broecker et al.* [1985] [*Hesshaimer et al.*, 1994], or concluded that in view of the large uncertainties of

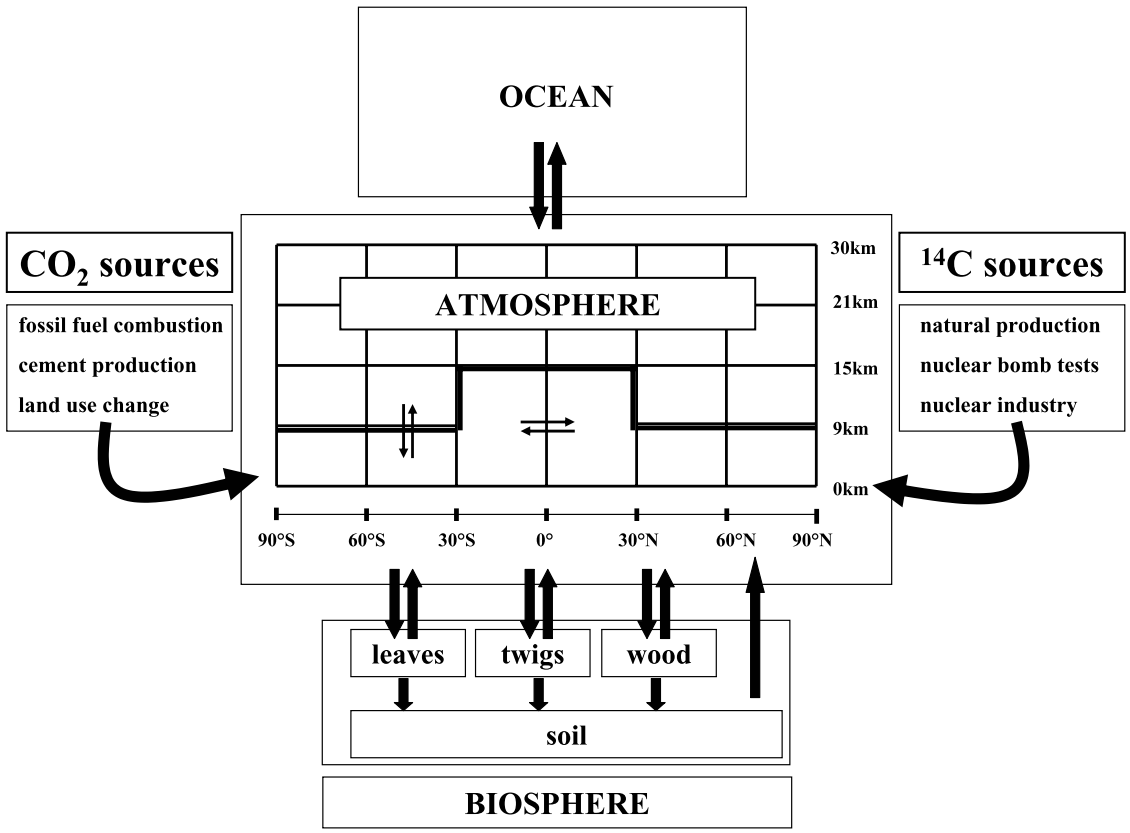

Figure 2. Structure of the GRACE model as used in this study. See text for details.

the observations, excess radiocarbon is not well-suited to confirm or to challenge our understanding of the global carbon cycle as a whole [*Jain et al.*, 1997]. However, today, new data sets like the bomb test compilation by *Yang et al.* [2000] are available. Also new, improved methods to separate the excess and the natural component in oceanic radiocarbon measurements have been developed [*Rubin and Key*, 2002; *Peacock*, 2004], allowing new estimates of the excess radiocarbon inventory in the ocean [*Peacock*, 2004; *Key et al.*, 2004]. Furthermore, improved simple carbon cycle models with well calibrated atmospheric transport [*Hesshaimer*, 1997; *Naegler*, 2005] have been developed. Finally, a thorough quality assessment of the stratospheric ^{14}C observations from the HASL reports [*Hesshaimer and Levin*, 2000; *Naegler*, 2005] narrowed the observational uncertainties and tightened the constraints imposed by the data. These new developments urge for a reevaluation of the global excess radiocarbon budget and our understanding of the global radiocarbon cycle, which is presented in this paper.

2. Methods

2.1. Model Description

[11] For this excess radiocarbon budget study, we used the GRACE (Global Radio Carbon Exploration) model originally developed by *Hesshaimer* [1997] and improved and described in detail by *Naegler* [2005]. Although the GRACE model has been developed as a (radio-) carbon cycle model (simulating all three carbon isotopes ^{12}C, ^{13}C, and ^{14}C), it additionally calculates atmospheric concentrations of tracers like SF_6 and the cosmogenic Beryllium isotopes ^{7}Be and ^{10}Be which are used for model transport calibration purposes (see below).

[12] The atmospheric part of the GRACE model consists of 22 boxes (six in the troposphere, 16 in the stratosphere) assumed to represent well-mixed zonal mean atmospheric compartments in six latitudinal subdivisions (see Figure 2). To keep the model as simple as possible, the exchange of air (and tracer) mass between adjacent atmospheric boxes is assumed to be purely diffusive. The time-dependent gross fluxes of air and any tracer from box i to the adjacent box j ($F_{air}^{i\to j}$, $F_{tracer}^{i\to j}$, respectively) are parameterized as

$$F_{air}^{i\to j}(t) = k_{ij}(t)\cdot m_i \tag{1}$$

$$F_{tracer}^{i\to j}(t) = F_{air}^{i\to j}(t)\cdot c_i(t) \tag{2}$$

where m_i denotes the air mass in box i, k_{ij} denotes the (seasonally variable) transport parameter for exchange between boxes i and j, and c_i denotes the (time-dependent) mass mixing ratio of the respective tracer in box i.

[13] The net airmass exchange between two adjacent boxes i and j is always assumed to be zero. Thus the (time-dependent) net exchange of tracer mass between these boxes is calculated as follows:

$$F_{tracer}^{ij,net}(t) = k_{ij}(t)\cdot m_i\cdot\left(c_i(t)-c_j(t)\right) \tag{3}$$

[14] We calibrated the seasonal atmospheric transport parameters k_{ij} with the parameter optimization tool MUSCOD-II [*Diehl*, 2002], using stratospheric and tropospheric radiocarbon observations between mid-1963 and 1970 [*Telegadas*, 1971; *Levin et al.*, 1985; *Berger et al.*, 1987; *Nydal and Lövseth*, 1996] and tropospheric SF_6 observations from 1988 to 1995 (*Maiss et al.* [1996] and unpublished Heidelberg data) as constraints. The seasonal cross-tropopause exchange in the southern extratropics was fine-tuned by eye with observations of the $^{10}Be/^{7}Be$ ratio (*Wagenbach* [1996] and updates by M. Huke, IUP Heidelberg, personal communication, 2004). Validation with independent SF_6 [*Harnisch et al.*, 1996; *Patra et al.*, 1997; *Strunk et al.*, 2000], CO_2 [*Etheridge et al.*, 1998; *GlobalView*, 2003; *Keeling and Whorf*, 2004] and $\delta^{13}C$ observations (*Mook et al.* [1983], *Francey and Allison* [1998], *Francey et al.* [1999], and *Allison et al.* [2003], and H. Meijer, Centrum voor Isotopenonderzoek (CIO) Groningen, personal communication, 2005) showed that the model is capable of simulating atmospheric transport and the cycling of carbon within the limits imposed by the coarse spatial resolution and the conceptional simplicity (see *Naegler* [2005] for details).

[15] The model atmosphere is coupled to a simple biosphere module which consists of four well-mixed carbon pools in each of the six latitudinal subdivisions of the model. The global biospheric carbon mass is 2200 PgC (1Pg = 10^{15}g), of which 53 PgC are assigned to a fast cycling pool (''leaves'') with a turnover time of τ = 2.5 years, 137 PgC are assigned to the ''twigs'' pool (τ = 6.5 years), 773 PgC are assigned to the ''wood'' pool (τ = 43.0 years) and 1238 PgC are assigned to almost immobile carbon in soils (τ = 610 years). Here 35% of a global total net primary production (NPP) of 60 PgC/yr are allocated to the ''leaves'' pool, 35% are allocated to the ''twigs,'' and 30% are allocated to the ''wood'' pool, respectively. The respiration of the ''soil'' pool is balanced by carbon input, in equal shares, from the ''leaves,'' ''twigs,'' and ''wood'' pools. These biospheric parameters (and other parameters such as isotopic fractionation, NPP allocation, biomass distribution on the latitudinal subdivisions, etc.) are consistent with earlier work [*Goudrian*, 1992; *Post*, 1993; *Mook*, 2000; *Olson et al.*, 2001]. To account for the isotopic disequilibrium between atmosphere and biosphere in prebomb times due to the Suess-Effect, the biospheric $\delta^{13}C$ and $\Delta^{14}C$ signatures for the begin of the model runs (in 1940) are taken from a spinup run where the model biosphere was driven with observed atmospheric $\delta^{13}C$ and $\Delta^{14}C$ between 1750 and 1940 [*Friedli et al.*, 1986; *Keeling et al.*, 1989; *Neftel et al.*, 1994; *Stuiver et al.*, 1998a, 1998b; *Francey et al.*, 1999; *Allison et al.*, 2003]. Details of the biosphere model are given by *Naegler* [2005].

[16] The model uses CO_2 fluxes from fossil fuel consumption and cement production according to *Marland et al.* [2003]. The isotopic composition of these CO_2 fluxes follows *Andres et al.* [1996]. Land-use change CO_2 fluxes are taken from *Houghton and Hackler* [2001]. To ensure that the modeled atmospheric CO_2 mixing ratio is consistent with the observations, the difference between the sum of anthropogenic emissions in the model (fossil fuel combustion, cement production, and land-use change) and the observed increase of the atmospheric CO_2 burden has to be taken up by the model ocean and biosphere. In the model, 45% of this uptake are allocated to the biosphere and 55% to the ocean, consistent with decadal budget estimates summarized by *Prentice et al.* [2001]. The allocation ratio is constant in time.

[17] In our GRACE model the radiocarbon flux between ocean and atmosphere (F_{14CO2}) is not modeled explicitly but is calculated from the observed $^{14}C/C$ ratio in the atmosphere and the ocean surface (R^A_{14}, R^O_{14}, respectively) and assumptions about the seasonally varying gross CO_2 flux from atmosphere to ocean (F^{AO}_G) (ocean to atmosphere (F^{OA}_G), respectively):

$$F_{^{14}CO_2} = F^{AO}_G \cdot R^A_{14} \cdot \alpha^{AO}_{14} - F^{OA}_G \cdot R^O_{14} \cdot \alpha^{OA}_{14}. \quad (4)$$

Here, α^{AO} and α^{OA} denote the kinetic fractionation factors for ^{14}C in CO_2 during the transfer from atmosphere to ocean and vice versa. We used (zonal mean) R^A_{14} and R^O_{14} histories reconstructed from available $\Delta^{14}C$ data in the atmosphere and the sea surface [*Hesshaimer*, 1997]. The gross carbon fluxes F^{AO}_G and F^{OA}_G consist of three components: First, the annual mean gross CO_2 flux F_G which is calculated as $F_G = N^A_C/\tau^{pre}_{AO}$ from estimates of the (preindustrial) atmospheric turnover time τ^{pre}_{AO} with respect to exchange with the ocean, and the (observed) atmospheric CO_2 content N^A_C. F_G is thus increasing with increasing N^A_C. Second, the (preindustrial) seasonal net CO_2 flux from *Heimann and Keeling* [1989], and third (in the case of F^{AO}_G), the net oceanic uptake of anthropogenic CO_2 whose calculation is described above. Note that the turnover time τ^{pre}_{AO} (and thus F^{AO}_G and F^{OA}_G) can be adjusted to fix the net radiocarbon uptake by the ocean in a way that the global radiocarbon budget is closed (see below).

2.2. Radiocarbon Sources in the Model

[18] The model contains all relevant sources of radiocarbon: bomb and natural ^{14}C production as well as the ^{14}C release by the nuclear industry. The natural radiocarbon production in the model depends on the scenario used (see below). It ranges between 0.48 kmol ^{14}C/yr ($2.9 \cdot 10^{26}$ atoms ^{14}C/yr) and 0.55 kmol ^{14}C/yr ($3.3 \cdot 10^{26}$ atoms ^{14}C/yr), averaged over a full 11-year solar cycle. The natural ^{14}C production varies around this average by ±10% between solar minimum and solar maximum. Natural radiocarbon production is distributed zonally and vertically according to *Lingenfelter* [1963]. Our estimate of the radiocarbon release by the nuclear industry follows *UNSCEAR* [1993], extrapolated to the end of the model simulation. For 2005, we thus estimated a ^{14}C release of 0.09 kmol ($0.57 \cdot 10^{26}$ atoms ^{14}C) by the nuclear industry.

[19] In the GRACE model we calculated the bomb radiocarbon production from the explosive force of atmospheric nuclear bomb tests as given by bomb test compilations and a constant bomb radiocarbon yield factor individually adjusted for each compilation (see below). The assumption of a constant yield factor may seem to be an oversimplification of the problem: *Glasstone and Dolan* [1977] report considerable variations in the neutron yield factor and the neutron energy spectrum not only with the type of nuclear fuel (^{235}U, ^{233}U, or ^{239}P for fission reactions, ^{2}H and ^{3}H ^{6}Li for fusion reactions, respectively) but also with the specific design of the bomb. They assume, though, a similar average neutron yield factor for fission and fusion bombs. On the basis of this assumption, *Enting*

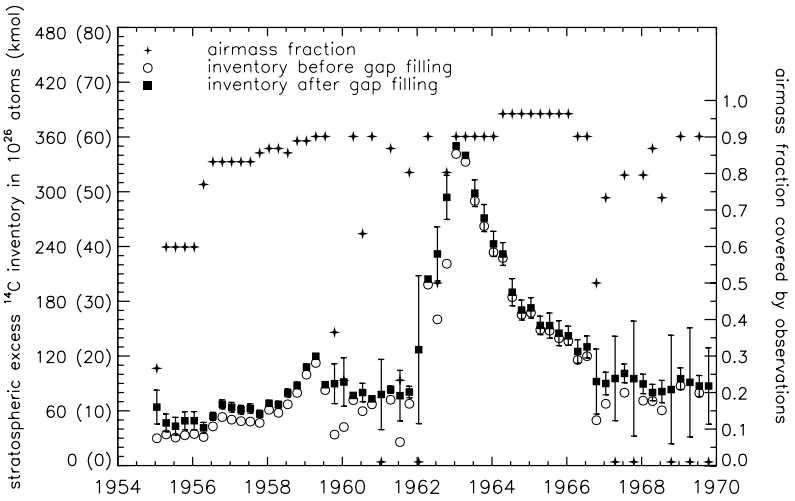

Figure 3. Stratospheric excess radiocarbon inventories before and after gap filling. (left) Stratospheric excess radiocarbon inventories before and after gap filling (open circles respectively filled squares). Units are 10^{26} atoms and (in parenthesis) kmol ^{14}C. (right) Fraction of stratospheric air mass covered by observations (stars).

[1982] estimated an average neutron yield factor for fission bombs of 1.0 to $4.0 \cdot 10^{26}$ neutrons per Mt TNT and 0.5 to $3.0 \cdot 10^{26}$ neutrons per Mt TNT for fusion bombs, with a most probable average yield of $2.0 \cdot 10^{26}$ neutrons per Mt TNT for fission and fusion bombs. In view of these large uncertainties and the lack of data to separately constrain the fission and fusion neutron (and thus radiocarbon) yield factors, we decided not to distinguish between fission and fusion bombs in this study but to follow the approach of *Glasstone and Dolan* [1977], *Enting* [1982], *Hesshaimer et al.* [1994], and *Lassey et al.* [1996] and assume the same radiocarbon yield factor for fission bombs as for thermonuclear bombs. When calculating the radiocarbon production of nuclear bomb tests, we further took into account that not all neutrons released in nuclear bomb tests produce radiocarbon. For example, for nuclear bomb tests close to the ground, a significant amount of the neutrons is absorbed by the Earth's surface [*Enting*, 1982], whereas for nuclear bomb tests in the stratosphere and mesosphere, a part of the neutrons escape into space. In both cases, no radiocarbon is produced. Depending on whether or not respective information was given in the bomb test compilation, we reduced the bomb radiocarbon yield of bomb tests close to the ground by 50% [*Enting*, 1982]. No corrections for high-altitude bombs were applied, as this correction is highly uncertain and only a small number of bombs were tested above the atmospheric boundary layer. The altitude of bomb radiocarbon injection into the atmosphere depends on the explosive force of the bomb tested. Here we use the parameterization of *Rath* [1988] to calculate the vertical extent of the bomb cloud which distinguishes between bomb tests in the tropics and extratropics to account for different average vertical stability of the atmosphere in high and low latitudes. Within the bomb cloud, bomb radiocarbon is distributed exponentially with altitude.

2.3. Calculation of Observed Atmospheric Excess Radiocarbon Inventories

[20] As described in detail by *Naegler* [2005], we calculated excess radiocarbon inventories (quarterly means) for the 16 stratospheric subdivisions of the GRACE model from atmospheric radiocarbon observations published in the HASL reports (see *Naegler* [2005] for a complete list of references). Our method follows closely the approach of *Hesshaimer and Levin* [2000] but takes into account increasing atmospheric CO_2 and decreasing atmospheric δ^{13}C. Radiocarbon inventories based on observations are not available for all stratospheric subdivisions of the model and not for all quarterly time steps. In the case of missing observations, we had to interpolate the data to obtain a complete coverage and to be able to calculate total stratospheric inventories. We first filled data gaps by interpolation in time and then by horizontal and vertical interpolation in space. The uncertainty estimate of the total stratospheric inventory increases depending on the amount of "gap filling" necessary at the respective time step. Details of this procedure can be found in the work of *Naegler* [2005]. Figure 3 shows the observed total stratospheric radiocarbon inventory (left axis) before (open circles) and after (filled squares) the gap filling process. The stars (right axis) depict the fraction of stratospheric air covered by observations. A high air mass fraction thus denotes little "gap filling" and therefore high reliability of the estimated stratospheric excess radiocarbon inventories in this period. Between early 1963 and September 1966, observational coverage is excellent (>90%), a possible bias in the total stratospheric inventory due to gap filling is respectively small during that period. As the radiocarbon yield factor in the model is calibrated using observed atmospheric inventories between August 1963 and August 1966 (see below), the yield factor depends only very little on the gap filling procedure.

[21] In addition to the HASL data, we evaluated stratospheric vertical Δ^{14}C, δ^{13}C, and CO_2 profiles observed over Japan in 1989 [*Nakamura et al.*, 1992] to obtain an additional stratospheric excess radiocarbon inventory estimate for 1989 (see Figure 4).

2.4. Scenarios for the Budget Study

[22] In order to assess the uncertainty of the global bomb ^{14}C production estimated in our model, we used the two extreme bomb radiocarbon input functions based on the

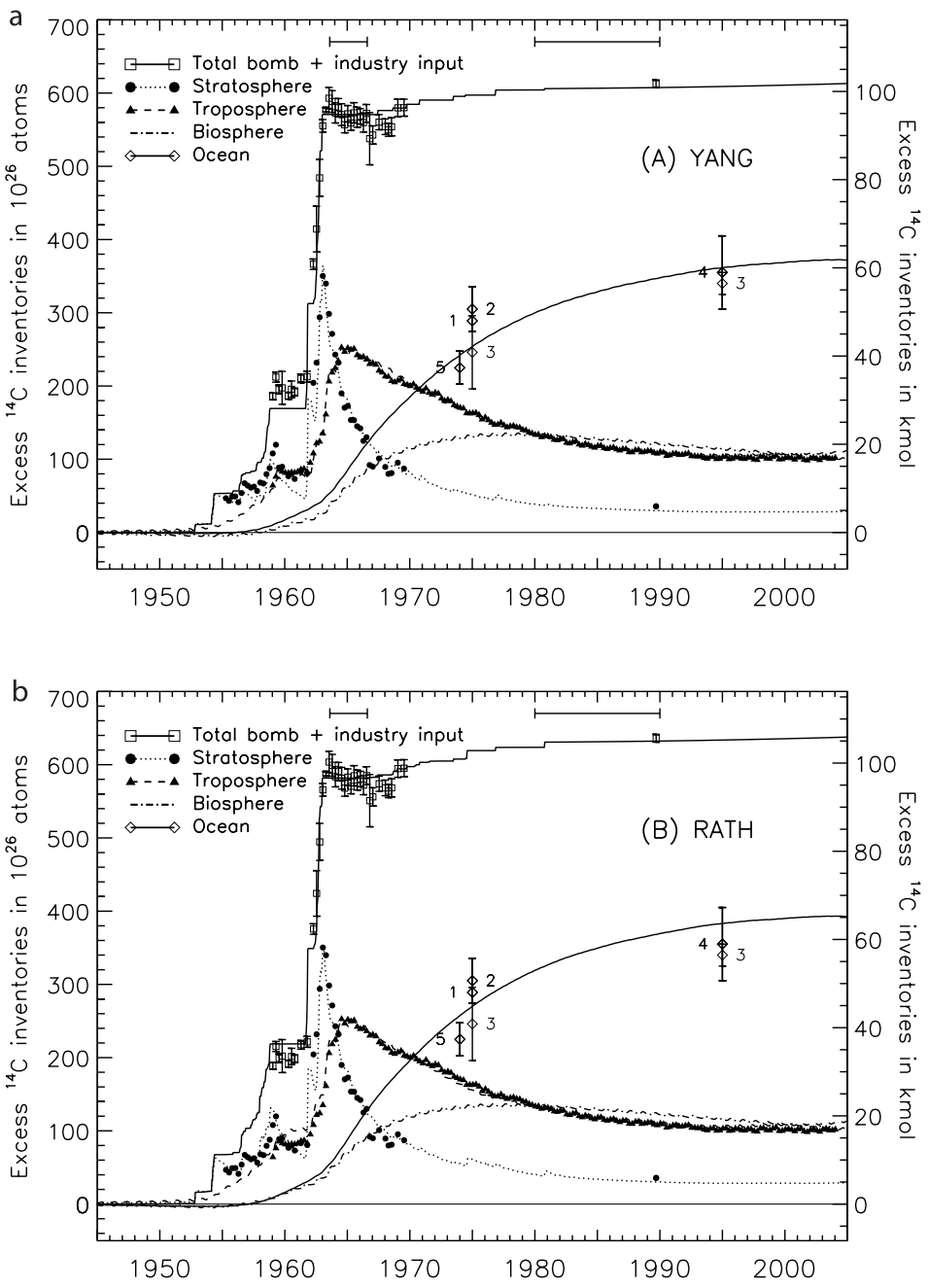

Figure 4. Modeled (lines) and observed (symbols) excess radiocarbon inventories for the compartments stratosphere (dotted line and circles), troposphere (dashed line and triangles), ocean (solid line and diamonds), and biosphere (dash-dotted line) in the scenarios (a) YANG and (b) RATH. Units are in 10^{26} atoms ^{14}C (left ordinate) and in kmol ^{14}C (right ordinate). The total cumulative radiocarbon input from nuclear bombs and the nuclear industry is shown as the solid line (histogram); the open squares denote the "observation-based total excess radiocarbon inventory" (see text). The respective uncertainties are dominated by the uncertainties of the stratospheric inventory, as the tropospheric uncertainties are small and uncertainties of the simulated biospheric and oceanic inventory are not taken into account. To keep the figure clear, uncertainties of the observed stratospheric and tropospheric inventories are not shown, but they are on the order of 1.7 kmol ^{14}C (10×10^{26} atoms ^{14}C) for the stratosphere in 1963 and on the order of less than a kmol ^{14}C (or a few 10^{26} atoms ^{14}C) for the troposphere. References for the observation-based ocean inventory estimates (diamonds): (1) *Broecker et al.* [1985], (2) *Broecker et al.* [1995], (3) *Peacock* [2004] (multitracer correlation method, corrected for missing ocean areas), (4) *Key et al.* [2004] (corrected for missing ocean areas). (5) denotes the result from *Hesshaimer et al.* [1994] based on a simple radiocarbon budget model. The two horizontal bars on top indicate the target periods for the calibration of the bomb yield factor (1963–1966) and the ocean-atmosphere turnover time τ_{AO}^{pre} (1980–1990, see text).

Table 3. Total Effective Explosive Force (TEEF), Bomb Radiocarbon Yield Factor, and Atmospheric Turnover Time With Respect to Ocean Exchange (τ_{AO}^{pre}) for the Different Scenarios[a]

	TEEF	Yield Factor ^{14}C Production/Mt TNT		τ_{AO}^{pre}
Scenario	Mt TNT	10^{26} Atoms	kmol	Years
YANG	352	1.72	0.286	11.1
YANGM5	352	1.70	0.282	11.7
RATH	598	1.06	0.176	10.1
RATHM5	598	1.04	0.173	10.6

[a]In contrast to the total explosive force shown in Figure 1, the total effective explosive force of the YANG and YANGM5 scenarios listed here is corrected for surface effects (see section 2.1).

bomb test compilations of *Yang et al.* [2000] and *Rath* [1988] (see Figure 1). Both compilations show different evolutions of the temporally integrated explosive force. These two compilations thus embrace our ignorance of the nuclear bomb tests' total explosive force and timing. Note that only the *Yang et al.* [2000], but not the *Rath* [1988] compilation, gives information about the altitude of the bomb tests. Therefore we reduced the radiocarbon production rate of bomb tests marked as "surface," "tower," and "barge" by 50% [*Enting*, 1982] in the *Yang et al.* [2000] bomb test compilation, but no surface corrections were applied to the *Rath* [1988] compilation.

[23] The quality of the stratospheric radiocarbon observations published in the HASL reports has long been debated. However, *Hesshaimer and Levin* [2000] and *Naegler* [2005] could show that the HASL data can not be biased toward higher values by more than 5% on average. However, this upper limit of a possible bias in the stratospheric excess radiocarbon observations has to be taken into account in our excess radiocarbon budget study which relies heavily on the observed stratospheric inventories. We therefore defined four different budget scenarios (see also Table 4): The scenario YANG uses the *Yang et al.* [2000] bomb test compilation and the original HASL data set. The scenario YANGM5 also uses the *Yang et al.* [2000] compilation, but the stratospheric excess ^{14}C inventories are reduced by 5%. RATH and RATHM5 denote the respective scenarios for the *Rath* [1988] bomb test compilation.

2.5. Calibration of the Radiocarbon Yield Factor and the Ocean-Atmosphere Turnover Time τ_{AO}^{pre} for Different Scenarios

[24] In the context of this study the model has two free parameters: First, the bomb radiocarbon yield factor (assumed to be constant over time) and second, the atmosphere-ocean turnover time τ_{AO}^{pre} for CO_2. We adjusted by eye in an iterative process both free model parameters simultaneously, separately for each scenario, according to two criteria which had to be met at the same time: First, the total modeled accumulated bomb radiocarbon production between August 1963 and August 1966 had to match the average "total observation-based excess radiocarbon inventory" at that time. Owing to the lack of time series of observed oceanic and biospheric excess radiocarbon inventories, the "total observation-based excess radiocarbon inventory" is defined as the sum of the observed stratospheric and tropospheric and the simulated oceanic and biospheric excess radiocarbon inventories. As a second criteria, the mean value of the simulated tropospheric excess radiocarbon inventories between 1980 and 1990 had to match the mean value of the observations within this period. The average absolute difference between quarterly mean simulated and observed tropospheric inventories between 1980 and 1990 for the different scenarios described above is less than 0.33 kmol ^{14}C (or $2 \cdot 10^{26}$ atoms ^{14}C). Note that we did not adjust the ocean inventory toward any observation-based ocean inventory estimate.

[25] We choose the first adjustment criteria and the first target period (August 1963 to August 1966) because first, there have not been any major atmospheric nuclear tests (>500 kt TNT) between January 1963 and October 1966. Second, from mid-1963 onward, the stratosphere seems to be well-mixed in a sense that no hot spots remained undetected by the HASL observations [*Naegler*, 2005], and third, data coverage in this period is best and thus the estimated total atmospheric inventories are the most reliable. The second criteria and the second target period were chosen because between 1980 and 1990, the troposphere is almost well mixed with respect to excess radiocarbon. Thus the tropospheric excess radiocarbon inventory is very well characterized by the available atmospheric $\Delta^{14}C$ observations. Furthermore, owing to the oversimplifying concept of a biosphere with four well-mixed pools, the simulated biospheric excess radiocarbon inventory probably becomes increasingly unrealistic from the early 1990s onward [see *Naegler*, 2005], affecting also simulated tropospheric excess radiocarbon inventories in the later years of our simulation. The solutions for the bomb radiocarbon yield factor and the ocean-atmosphere turnover time τ_{AO}^{pre} (Table 3) appear to be independent on the starting values of our iterative adjustment process. Our estimates of τ_{AO}^{pre} are higher than previous estimates [e.g., *Oeschger et al.*, 1975; *Broecker et al.*, 1985]. Our findings thus imply a smaller air-sea gas exchange rate and a lower gross CO_2 exchange flux between ocean and atmosphere. These results are consistent with the fact that our modeled ocean excess radiocarbon inventory agrees well with the (corrected) observed inventories from *Peacock* [2004] and *Key et al.* [2004], which are lower than earlier estimates of the ocean excess radiocarbon inventory from *Broecker et al.* [1985] and which have been used to constrain air-sea gas exchange and the gross CO_2 exchange flux so far [*Broecker et al.*, 1985; *Wanninkhof*, 1992]. A detailed discussion of the consequences of the new ocean excess radiocarbon inventories for air-sea gas exchange can be found in the work of *Naegler et al.* [2006].

3. Results

[26] Resulting bomb radiocarbon yield factors and total bomb radiocarbon production for the four different scenarios are summarized in Table 4. The differences in the bomb ^{14}C yield factors for the RATH and the YANG scenario reflect the differences in the total explosive force of atmospheric nuclear bomb tests in both compilations, the higher the total explosive force, the lower the yield factor (see Figure 1). Estimates of the total bomb radiocarbon production range from 99.3 kmol ^{14}C ($598 \cdot 10^{26}$ atoms ^{14}C, YANGM5) to 104.9 kmol ^{14}C ($632 \cdot 10^{26}$ atoms ^{14}C, RATH). Figure 4a shows the modeled and observed strato-

Table 4. Total Anthropogenic Radiocarbon Input (in kmol, 10^{26} Atoms ^{14}C, Respectively) and Simulated Excess Radiocarbon Inventories (in kmol ^{14}C, 10^{26} Atoms ^{14}C, Respectively) for the Different Scenarios (and, if Available, the Corresponding Observations, OBS) on January 1975 (Midpoint GEOSECS) and January 1995 (Midpoint WOCE)[a]

	Total Input		Stratosphere		Troposphere		Biosphere		Ocean	
Scenario	1975	1995	1975	1995	1975	1995	1975	1995	1975	1995
					Units in kmol ^{14}C					
YANG	99.2	101.1	8.6	4.7	26.8	17.5	21.7	18.9	42.1	60.0
YANGM5	97.8	99.8	8.4	4.7	26.6	17.7	22.2	19.2	40.7	58.1
RATH	102.8	105.2	10.1	4.7	25.9	17.6	22.1	19.2	44.9	63.6
RATHM5	100.5	102.9	9.9	4.8	25.7	17.7	22.0	19.2	43.0	61.2
OBS					27 ± 1	17 ± 1			40.7–56.5	43.8–59.0
					Units in 10^{26} Atoms ^{14}C					
YANG	597.2	609.0	51.9	28.2	161.5	105.5	130.9	113.6	253.7	361.5
YANGM5	589.0	600.7	50.7	28.4	160.4	106.3	133.7	115.9	245.1	350.0
RATH	619.2	633.6	61.1	28.6	155.8	106.2	133.0	115.6	270.1	383.2
RATHM5	605.5	619.7	59.6	28.7	155.0	106.8	132.5	115.9	259.1	368.3
OBS					163 ± 5	105 ± 5			245–264	340–355

[a]The total anthropogenic input comprises production from bomb tests and nuclear industry and is corrected for decay between the time of production of the radiocarbon and 1975 and 1995, respectively. The observed ocean inventory (OBS) is the range of estimates from *Peacock* [2004] (multitracer regression and corrected silicate methods, not including her error estimates, but corrected for missing ocean areas) and *Key et al.* [2004] (corrected for missing ocean areas).

spheric, tropospheric, biospheric, and oceanic excess radiocarbon inventories as well as the total cumulated bomb radiocarbon production and the ''total observation-based inventory'' for the YANG scenario. Quarterly mean modeled excess radiocarbon inventories and the cumulated production are shown as lines; the symbols denote the observations (see figure legend and caption for details).

[27] In general, the model matches the observed tropospheric inventories very well. Minor discrepancies appear in 1968, where modeled inventories are systematically higher than the observations by up to 2.5 kmol ^{14}C ($15 \cdot 10^{26}$ atoms ^{14}C). After 1995, there is a tendency in the modeled tropospheric inventory to again overestimate the radiocarbon content. In the stratosphere, the model simulates the observed inventories after 1962 very well. Before 1962, however, the model systematically underestimates the observed inventories by up to 30%. The modeled ocean excess radiocarbon inventories in the YANG scenario are 42.2 kmol ^{14}C ($254 \cdot 10^{26}$ atoms ^{14}C) in 1975 (GEOSECS) and 60.1 kmol ^{14}C ($362 \cdot 10^{26}$ atoms ^{14}C) in 1995 (WOCE, see Table 4). The YANG result for GEOSECS agrees, within 1σ, well with the estimates from *Hesshaimer et al.* [1994] and *Peacock* [2004] (see Table 4). However, it does not match the results from *Broecker et al.* [1995] within the uncertainties, nor the results from *Broecker et al.* [1985], where no uncertainty estimates are given. For the time of WOCE, the model results are consistent (within the uncertainties) with the (corrected, see above) results from *Peacock* [2004] and *Key et al.* [2004].

[28] During the periods when no bomb tests took place (November 1958 to August 1961, January 1963 to May 1967, and after 1980), the ''observed'' total excess radiocarbon inventory is expected to be constant (as the input from the nuclear industry is negligible during these periods). During the first moratorium (late 1958 until mid-1961), the YANG scenario underestimates the observed total excess radiocarbon inventory by 14%. Within the large scatter, the ''observed'' total excess inventory is constant. However, during the second moratorium, the ''observed'' total excess inventory decreases slightly (-0.85 ± 0.45 kmol ^{14}C per year or $-5.1 \pm 2.7 \cdot 10^{26}$ atoms ^{14}C/year). As the bomb yield factor and thus the total production of bomb radiocarbon is calibrated against the average ''observed'' total excess inventory during the second moratorium, the model matches the average ''observed'' total excess inventory between late 1963 and late 1966 very well.

[29] The results for the RATH scenario are qualitatively similar (Figure 4b). However, in contrast to the YANG scenario, the RATH scenario simulates well the stratospheric excess radiocarbon inventory before 1962, whereas the tropospheric inventory is overestimated by up to 20% during this time. Furthermore, the model tends to slightly underestimate the tropospheric inventory between 1971 and 1981. The excess radiocarbon inventory in the ocean is larger in the RATH scenario than in the YANG scenario (see Table 4). While for GEOSECS, the model is still compatible with the estimates from *Broecker et al.* [1995] and *Peacock* [2004] within their uncertainties, the model predicts a significantly higher inventory than *Hesshaimer et al.* [1994]. The simulated ocean inventory is lower than the estimate from *Broecker et al.* [1985], but no uncertainties are given here. For WOCE, the modeled inventory is, within 1σ of the observations' uncertainties, not compatible with the corrected estimates from *Peacock* [2004], but agrees within the uncertainties with the corrected inventory from *Key et al.* [2004]. During the first moratorium, the RATH scenario overestimates the ''observed'' total excess radiocarbon inventory by 8%. During the second moratorium, the total ''observed'' excess radiocarbon inventory also decreases slightly (-0.70 ± 0.45 kmol ^{14}C per year or $-4.2 \pm 2.7 \cdot 10^{26}$ atoms ^{14}C/year).

[30] According to the reduced observed stratospheric excess radiocarbon inventory in the scenarios YANGM5 and RATHM5 (Figures not shown), the total anthropogenic radiocarbon production necessary to match the observations is reduced, too. Consequently, the uptake in the reservoirs ocean and biosphere is smaller. Qualitatively, the YANGM5 scenario exhibits the same flaws as the YANG scenario (stratospheric inventories before 1962 too low, overestimation of tropospheric inventory in 1967–1969). The same is true for the RATHM5 and the RATH scenario (tropospheric inventories before 1962 too high and too low between 1971

and 1981). A summary of the modeled and observed inventories for the time of GEOSECS and WOCE for all scenarios can be found in Table 4.

4. Discussion

[31] Despite the overall very good agreement between modeled and observed excess radiocarbon inventories, a number of striking differences between model and observations need to be discussed. We will focus here on the YANG and RATH scenarios, as the YANGM5 and the RATHM5 scenario results are qualitatively similar to the YANG and the RATH case, respectively.

4.1. Differences in Simulated and Observed Atmospheric Excess ^{14}C Inventories Before 1962

[32] Before 1962, the model does not simultaneously satisfactorily simulate both the stratospheric and the tropospheric inventory, neither in the YANG nor the RATH scenario. While the YANG scenario simulates tropospheric excess radiocarbon well, the RATH scenario simulations match the stratospheric observations better. A number of factors could be responsible for this mismatch: First, the *Yang et al.* [2000] bomb test compilation could overestimate the relative strengths of nuclear bomb tests (and thus the bomb ^{14}C production) until late 1958, while the Rath compilation underestimates relative strengths of the early tests. However, as the injection altitude of bomb ^{14}C depends on the amount of energy released in the blast and thus on the bomb strength, a redistribution of the total explosive force between the periods before and after the first moratorium would redistribute the released ^{14}C between stratosphere and troposphere, thus reducing the good agreement between model and observations before 1960 in the troposphere (YANG) and stratosphere (RATH), respectively.

[33] Second, the assumption of a single radiocarbon yield factor for all nuclear bomb tests could oversimplify the situation. If the bomb ^{14}C production is calculated with a different yield factor for bombs before 1958 (the first test stop) and after 1958 (e.g., owing to the technological evolution of nuclear bombs between the 1950s and the 1960s, e.g., a the shift from fission bombs in the early 1950s to thermonuclear bombs in the late 1950s and 1960s), the RATH scenario would require a lower yield factor in the early years, whereas the YANG scenario calls for a higher yield factor. As mentioned above, following *Glasstone and Dolan* [1977], we assume identical yield factors for fission and fusion reactions. However, in view of the range of uncertainties *Glasstone and Dolan* [1977] give for the neutron yield factor (50–200% for fission and 25–150% for fusion), we assume that, given there is a difference between the fission and fusion yield factor, the yield factor for thermonuclear bombs is rather expected to be smaller than that for fission bombs (at the same explosive force). This would mean that we underestimate the bomb radiocarbon production in the early 1950s, when fission bombs prevail. Thus the underestimation of the total bomb radiocarbon inventory before 1962 in the YANG scenario could at least qualitatively be explained by the justifiable assumption of a lower radiocarbon yield of thermonuclear bombs with respect to fission bombs. However, the RATH scenario requires the contrary assumption to explain the data-model mismatch. In this context it is also important to note that a small number of bombs with very high explosive force dominate the total radiocarbon production. In the *Yang et al.* [2000] compilation, the ten strongest nuclear bomb tests make up 40% of the total explosive force of all atmospheric bomb tests. If the neutron (and thus radiocarbon) production rate of one of these tests differed considerably from the average production rate assumed to be valid for all tests in the model, the model would not be capable of simulating correctly the observed excess radiocarbon inventories. For example, if the neutron production rate of the strongest nuclear bomb test (a Sowjet test of 50Mt TNT in October 1961 [*Yang et al.*, 2000]) was lower than the average production rate assumed, the model would underestimate the total bomb radiocarbon production before that test. So the assumption of a below-average radiocarbon production rate for this test (or any other strong test of the 1961–1962 test series) could explain the model-data differences in the YANG scenario. Again, however, the RATH scenario requires the opposite assumption.

[34] Third, atmospheric excess ^{14}C inventories, could be significantly biased before 1962. The YANG scenario would require that observed stratospheric inventories are biased toward higher values, whereas the RATH simulation could be reconciled with higher tropospheric observations. However, as tropospheric $\Delta^{14}C$ measurements before 1963 were made in high-precision laboratories and have been subject to regular quality control and interlaboratory comparison, a bias in the tropospheric data is unlikely. A comparison of simulated and observed stratospheric inventories for each hemisphere (not shown) indicates that the YANG scenario underestimates the stratospheric inventory mainly in the Southern Hemisphere. As shown by *Naegler* [2005], it is possible that the stratospheric observations in the southern hemisphere from the HASL reports are slightly biased toward higher values, whereas the northern hemispheric observations are not. Thus a contamination of the HASL sampling device in the Southern Hemisphere could be held responsible for the apparent underestimation of the stratospheric excess ^{14}C inventory in the YANG case. If this assumption was true, the RATH scenario would overestimate both the stratospheric and the tropospheric inventory, which could be explained by the overestimation of the relative strength of the early bombs in the *Rath* [1988] compilation.

4.2. Apparently Decreasing Total Observation-Based Inventory in 1963–1966

[35] In both the YANG and the RATH scenarios, the ''observed'' total excess radiocarbon inventory (open squares in Figure 4) slightly decreases between late 1963 and late 1966. As we expect a constant total inventory due to radiocarbon mass conservation and negligible radioactive decay in this period, a decreasing total ''observed'' inventory points out a ''hidden'' radiocarbon sink not accounted for in our model. For example, a (small) underestimation of the biospheric or oceanic excess radiocarbon uptake between 1963 and 1966 would account for this sink (see below). Our finding is in contradiction with results from *Telegadas and List* [1969], *Chang* [1976], *Johnston* [1989], and *Broecker and Peng* [1994], who rather inferred a

"hidden bomb ^{14}C source" from their analyses of the HASL data. However, our findings here are consistent with recent analyses from *Hesshaimer and Levin* [2000] and *Naegler* [2005], who showed that a "hidden source" in the stratosphere is not likely after mid-1963 when the observations from the HASL report are representative for the large-scale distribution of excess radiocarbon in the stratosphere. The small apparent "hidden sink" found in our simulations could be explained by the following assumptions:

[36] First, the simulated temporal evolution of the oceanic and biospheric inventories during the mid to late 1960s could be wrong. If the biospheric and oceanic radiocarbon uptake in the model would be stronger in the late 1960s (and respectively weaker after 1970), the decrease in the total "observed" excess radiocarbon inventory would vanish. As the shape (until the mid-1970s) of the oceanic excess radiocarbon inventory from this study is similar to independent ocean model simulations from *Hesshaimer et al.* [1994], *Duffy and Caldeira* [1995], and K. Rodgers (Laboratoire d'Océanographie Dynamique et de Climatologie (LODYC), Paris, personal communication, 2004) and the total inventory at the time of GEOSECS is consistent with recent observation-based estimates from *Peacock et al.* [2004] and *Key et al.* [2004], we assume our simulated ocean excess radiocarbon inventory can probably not be held responsible for the decrease of the total "observed" excess radiocarbon inventory in the 1960s. On the other hand, as already pointed our by *Joos* [1994] and *Jain et al.* [1997], simulated biospheric excess radiocarbon inventories depend strongly on model parameters such as turnover times, NPP, pool sizes, etc., so that it is plausible to assume that the model biosphere underestimates the biospheric excess radiocarbon inventory in the middle and late 1960s.

[37] Second, the apparent "hidden sink" could be explained if the observed stratospheric excess radiocarbon inventories were overestimated by around 15%. If corrected for this possible bias, the absolute reduction of stratospheric inventories in the early 1960s is larger than in the late 1960s, leveling off the total "observed" excess radiocarbon inventory. However, as *Hesshaimer and Levin* [2000] and *Naegler* [2005] already have shown, a possible bias in the stratospheric radiocarbon observations is less than 5% and could thus explain only parts of the "hidden sink."

4.3. Increasing Simulated Tropospheric Excess ^{14}C Inventories in the 1990s

[38] The model simulates increasing tropospheric excess ^{14}C inventories in the late 1990s, in contradiction to the observations, which show a rather constant tropospheric inventory since about 1995. In the late 1990s, the model ocean is almost in ^{14}C equilibrium with the atmosphere, resulting in small net excess radiocarbon uptake, whereas the model biosphere is a source of radiocarbon to the atmosphere after the middle to late 1970s. The mismatch between modeled and observed tropospheric excess radiocarbon inventories could be explained if the model biosphere overestimated this ^{14}C source (owing to an inadequate setup or parameterization of the biosphere module) or if the model ocean underestimates the radiocarbon uptake in the late 1990s (owing to weak data constraints of sea surface $\Delta^{14}C$ after the WOCE survey (mid-1990s)). A continuing record of atmospheric $\Delta^{14}C$ as well as new ocean surface $\Delta^{14}C$ data for the early 21st century would be desirable to test the performance of the model ocean and the biosphere.

4.4. Comparison of Simulated and Observed Ocean Excess ^{14}C Inventories

[39] Our estimates of the ocean excess radiocarbon inventory range from 40.7 to 44.8 kmol ^{14}C (245 to 270 $\cdot$ 10^{26} atoms ^{14}C) for GEOSECS and from 58.1 to 63.6 kmol ^{14}C (350 to 383 $\cdot$ 10^{26} atoms ^{14}C) for WOCE (Table 4). They are slightly higher (but consistent within the uncertainties) than recent observation-based ocean excess radiocarbon inventory estimates of 40.7 kmol ^{14}C (245 $\cdot$ 10^{26} atoms ^{14}C) for GEOSECS [*Peacock*, 2004] and 56.5–59.0 kmol ^{14}C (340–355 $\cdot$ 10^{26} atoms ^{14}C) for WOCE (corrected by *Naegler* [2005, see Table 2], *Peacock* [2004], *Key et al.* [2004]). However, as already mentioned above, the modeled excess radiocarbon inventory of the terrestrial biosphere depends strongly on the biosphere model setup and parameterization. Thus it is possible that we underestimate the simulated biospheric excess radiocarbon inventory. As simulated atmospheric inventories are "fixed" by the observations via parameter adjustment, this deficit would be assigned to the model ocean in our analysis, resulting in an overestimation of the ocean excess radiocarbon inventory.

4.5. Discussion of Uncertainties

[40] Two main factors contribute to the uncertainties in our estimates of the total bomb radiocarbon production: the different temporal behavior of the cumulative explosive force of nuclear bombs after 1963 and uncertainties in the "total observation-based excess radiocarbon inventory" in the 1963–1966 calibration period. Uncertainties in the "total observation-based excess radiocarbon inventory," in turn, are caused by uncertainties in the observed stratospheric and tropospheric excess radiocarbon inventories and possible errors in the simulated excess radiocarbon inventories in the ocean and the biosphere during that time. Uncertainties in the cumulative explosive force have been taken into account by our use of two very different bomb test compilations. Uncertainties of the observed tropospheric excess radiocarbon inventories are small, thanks to numerous high-precision $\Delta^{14}C$ measurements. Uncertainties in the stratospheric inventories are dominated by the possible systematic bias in the HASL data, which has been taken into account by repeating our simulations with HASL radiocarbon data reduced by 5%. During the August 1963 to August 1966 period, biospheric and oceanic excess radiocarbon inventories are still small (less than 16.6 kmol ^{14}C or 100 $\cdot$ 10^{26} atoms ^{14}C), so that an estimated error of probably less than 10% in the simulated oceanic and biospheric inventories introduces only a small error (less than 2.5 kmol ^{14}C or 15 $\cdot$ 10^{26} atoms ^{14}C, which is less than 2%) in the "total observation-based excess radiocarbon inventory" and in the respective bomb radiocarbon yield factor. Thus the range of uncertainty in the total bomb radiocarbon production is largely encompassed by the range of our estimates for the different scenarios given in Table 3.

[41] In contrast, the range of ocean excess radiocarbon inventories simulated for the four different scenarios discussed here (Table 4) only gives a lower estimate of the uncertainty of this quantity, taking into account only uncer-

tainties in the bomb radiocarbon production. For each scenario, however, the simulated ocean excess radiocarbon inventory depends also on the simulated stratospheric, tropospheric, and biospheric inventory. While the simulated tropospheric excess radiocarbon inventory agrees well with the observations until the late 1990s and the simulated stratospheric inventories also match well the only data point after 1970 (from 1989, see Figure 4), considerable uncertainty persists about the biospheric excess radiocarbon inventory (and in consequence, about the ocean excess radiocarbon inventory). Tests with the GRACE biosphere module [*Naegler*, 2005] have shown that the simulated biospheric excess radiocarbon inventory is particularly sensitive to changes of the biospheric carbon turnover times and the NPP allocation. *Naegler* [2005] estimates the associated uncertainty of the biospheric inventory to be up to 15% for the mid-1970s (3.3 kmol or $20 \cdot 10^{26}$ atoms ^{14}C) and up to 20% for the mid-1990s (3.8 kmol or $23 \cdot 10^{26}$ atoms ^{14}C). Furthermore, the more realistic consideration of a finite residence time of assimilated carbon in living biomass by biosphere modules of lagged-response type [*Hesshaimer*, 1997] leads to a significant increase of the biospheric excess radiocarbon inventory compared to biosphere modules of well-mixed type [*Naegler*, 2005]. Therefore we assume that we underestimate rather than overestimate the biospheric excess radiocarbon inventory simulated with our well-mixed biosphere module (and, in consequence, rather overestimate the ocean inventory). However, even taking these additional uncertainties into account, we still expect our simulated ocean excess radiocarbon inventories to match the (corrected) inventory estimates from *Peacock* [2004] and *Key et al.* [2004] within their uncertainties. A further quantitative assessment of the uncertainties of the simulated oceanic and biospheric excess radiocarbon inventories is difficult and would require additional observational constraints.

4.6. Discussion of Previous Global Excess Radiocarbon Budget Studies

[42] A number of previous studies have tried to close the global excess radiocarbon budget, but most of them failed because they assumed too low stratospheric or too high ocean excess radiocarbon inventories: *Broecker and Peng* [1994] found a serious mismatch in the global excess ^{14}C budget because they had fixed their model ocean to an inventory of 58.1 kmol ^{14}C ($350 \cdot 10^{26}$ atoms ^{14}C) in 1975, which is more than 30% higher than current estimates from *Peacock* [2004] (40.7–43.8 kmol ^{14}C or $245–264 \cdot 10^{26}$ atoms ^{14}C). A downward revision of their inventory estimates to 50.6 kmol ^{14}C ($305 \cdot 10^{26}$ atoms ^{14}C) [*Broecker et al.*, 1995] decreased the mismatch, but they still concluded (spuriously) that the stratospheric data from the HASL reports were not reliable before 1965. *Hesshaimer et al.* [1994] revised the HASL data downward by 16.5% to account for the criticism of *Tans* [1981]. As *Hesshaimer et al.* [1994] used the revised HASL data to calibrate their bomb radiocarbon yield factor, their bomb ^{14}C production (for the *Rath* [1988] bomb compilation) is lower than our respective results. Consequently, they balanced their lower bomb ^{14}C production with a lower ocean excess radiocarbon inventory (37.2 kmol ^{14}C or $224 \cdot 10^{26}$ atoms ^{14}C for 1974). If they had used the original HASL data, they had thus obtained an ocean excess radiocarbon inventory close to our value. Owing to the lack of stratospheric constraints, the model of *Lassey et al.* [1996] managed to "close" the global excess radiocarbon budget, even though they assumed an ocean excess ^{14}C inventory value for GEOSECS of 54.6–60.1 kmol ^{14}C ($329–362 \cdot 10^{26}$ atoms ^{14}C), much higher than recent estimates from *Peacock* [2004]. Similar to the study by *Hesshaimer et al.* [1994], *Jain et al.* [1997] used the downwardly revised HASL data, leading to too low stratospheric inventories. Furthermore, they simulated an ocean excess radiocarbon inventory (54.1 kmol ^{14}C or $326 \cdot 10^{26}$ atoms ^{14}C for 1975) which is too high compared to the results from *Peacock* [2004]. *Jain et al.* [1997] concluded that in view of the large uncertainties of the excess ^{14}C observations and the bomb ^{14}C production rate, excess radiocarbon would not impose any constraints on our understanding of the global carbon cycle.

5. Conclusions

[43] In this study, we simulated the global cycle of radiocarbon with the simple global (radio-) carbon cycle model GRACE. With the help of the GRACE model, available stratospheric and tropospheric radiocarbon observations, and four different compilations of atmospheric nuclear bomb tests, we estimated the global production of bomb radiocarbon between 1945 and 1980 to be 99.3–104.9 kmol ^{14}C ($598–632 \cdot 10^{26}$ atoms ^{14}C). Our study shows, for the very first time, that it is possible to simulate excess radiocarbon inventories in the main carbon reservoirs in good to excellent agreement with all available data. We are thus able to close the global budget of excess radiocarbon within the limits of our present understanding of the global carbon cycle. Furthermore, we confirm, with a totally independent approach, the observation-based ocean excess radiocarbon inventory estimates for the time of GEOSECS [*Peacock*, 2004] and WOCE [*Peacock*, 2004; *Key et al.*, 2004] (original estimates corrected for missing ocean areas by *Naegler* [2005]). However, this finding also implies that the ocean excess ^{14}C inventory estimate from *Broecker et al.* [1985] is not consistent with our current knowledge of the global excess radiocarbon budget. As the *Broecker et al.* [1985] estimate has been used to calibrate the widely employed air-sea gas exchange formulation from *Wanninkhof* [1992], our findings call for a reevaluation of the excess radiocarbon constraints on air-sea gas exchange and the uptake of CO_2 by the oceans [see *Naegler et al.*, 2006]. Similarly important, our excess ^{14}C budget study now provides for the very first time an indirect but data-based estimate of the biospheric excess radiocarbon inventory. This can be used as an important new constraint for the setup and parameterization of global biosphere models [see *Naegler*, 2005].

[44] **Acknowledgments.** We thank Synte Peacock for sharing her data with us, Keith Rodgers for helpful discussions on oceanic radiocarbon exchange, Xiaoping Yang for helpful clarifications concerning the CMR nuclear explosions database, and especially Philippe Ciais for helpful discussions and the LSCE for financial support. We also thank the two reviewers Ken Caldeira and Ian Enting whose comments helped to improve the manuscript. This work would not have been possible without the invaluable pioneering work by Vago Hesshaimer who developed an earlier version of the GRACE model and has set the stage for our recent simulations. His contribution is gratefully acknowledged.

References

Allison, C. E., R. Francey, and P. Krummel (2003), $\delta^{13}C$ in CO_2 from sites in the CSIRO Atmospheric Research GASLAB air sampling network (April 2003 version), in *Trends: A Compendium of Data on Global Change*, Carbon Dioxide Inf. Anal. Cent., Oak Ridge Natl. Lab., Oak Ridge, Tenn.

Andres, R. J., G. Marland, and S. Bischof (1996), Global and latitudinal estimates of ^{13}C from fossil-fuel consumption and cement manufacture, *Data Rep. db1013*, Carbon Dioxide Inf. Anal. Cent., Oak Ridge Natl. Lab., Oak Ridge, Tenn.

Berger, R., T. B. Jackson, R. Michael, and H. E. Suess (1987), Radiocarbon content of tropospheric CO_2 at China Lake, California 1977-1983, *Radiocarbon*, *29*, 18–23.

Broecker, W. S., and T.-H. Peng (1994), Stratospheric contribution to the global bomb radiocarbon inventory: Model versus observations, *Global Biogeochem. Cycles*, *8*, 377–384.

Broecker, W. S., T.-H. Peng, and R. Engh (1980), Modelling the carbon system, *Radiocarbon*, *22*, 565–598.

Broecker, W. S., T.-H. Peng, G. Östlund, and M. Stuiver (1985), The distribution of bomb radiocarbon in the ocean, *J. Geophys. Res.*, *90*, 6953–6970.

Broecker, W. S., S. Sutherland, W. Smethie, T.-S. Peng, and G. Östlund (1995), Oceanic radiocarbon: Separation of the natural and bomb component, *Global Biogeochem. Cycles*, *9*, 263–288.

Chang, J. (1976), Uncertainties in the validation of parameterized transport in 1-D models of the stratosphere, in *Proceedings of the Fourth Conference on the Climatic Impact Assessment Program*, edited by T. M. Hard and A. J. Broderick, pp. 368–380, Dept. of Trans., Washington D.C.

Diehl, M. (2002), Real-time optimization for large scale nonlinear processes, in *Fortschr.-Ber. VDI Reihe 8, Meß-, Steuerungs- und Regelungstechnik*, vol. 920, VDI Verlag, Düsseldorf. (Available at http://www.ub.uni-heidelberg.de/archiv/1659/)

Duffy, P. B., and K. Caldeira (1995), Three-dimensional model calculation of ocean uptake of bomb ^{14}C and implications for the global budget of ^{14}C, *Global Biogeochem. Cycles*, *9*, 373–375.

Enting, I. (1982), Nuclear weapons data for use in carbon cycle modelling, *Tech. Pap. 44*, CSIRO Div. of Atmos. Res., Melbourne, Australia.

Enting, I., and G. I. Pearman (1982), Description of a one-dimensional global carbon cycle model, *Tech. Pap. 42*, CSIRO Div. of Atmos. Res., Melbourne, Australia.

Etheridge, D., L. Steele, R. Langenfelds, R. Francey, J.-M. Barnola, and V. Morgan (1998), Historical CO_2 records from the Law Dome DE08, DE08-2, and DSS ice cores, in *Trends: A Compendium of Data on Global Change*, Carbon Dioxide Inf. Anal. Cent., Oak Ridge Natl. Lab., Oak Ridge, Tenn.

Francey, R., and C. E. Allison (1998), In situ carbon 13 and oxygen 18 ratios of atmospheric CO_2 from Cape Grim, Tasmania, Australia: 1982-1993, in *Trends: A Compendium of Data on Global Change*, Carbon Dioxide Inf. Anal. Cent., Oak Ridge Natl. Lab., Oak Ridge, Tenn.

Francey, R. J., C. Allison, D. Etheridge, C. Trudinger, I. Enting, M. Leuenberger, R. Langenfelds, E. Michel, and L. Steele (1999), A 1000 year high precision record of $\delta^{13}C$ in atmospheric CO_2, *Tellus, Ser. B*, *51*, 170–193.

Friedli, H., H. Lötscher, H. Oeschger, U. Siegenthaler, and B. Stauffer (1986), Ice core record of $^{13}C/^{12}C$ ratio of atmospheric CO_2 in the past two centuries, *Nature*, *324*, 237–238.

Glasstone, S., and P. J. Dolan (1977), *The Effects of Nuclear Weapons*, U.S. Dept. of Defense and the Energy Res. and Dev. Admin., Washington D. C. (Available at http://www.princeton.edu/~globsec/publications/effects/effects.shtml)

GlobalView (2003), Cooperative atmospheric data integration project—Carbon dioxide, *Tech. Rep.*, NOAA CMDL, Boulder, Colo. (Available at ftp.cmdl.noaa.gov, path: ccg/CO2/GLOBALVIEW)

Goudrian, J. (1992), Biosphere structure, carbon sequestering potential and the atmospheric ^{14}C record, *J. Exp. Botany*, *43*, 1111–1119.

Harnisch, J., R. Borchers, P. Fabian, and M. Maiss (1996), Tropospheric Trends for CF_4 and C_2F_6 since 1982 from SF_6 dated stratospheric air, *Geophys. Res. Lett.*, *32*, 1099–1102.

Heimann, M., and C. D. Keeling (1989), A three-dimensional model of atmospheric CO_2 transport based on observed winds: 2. Model description and simulated tracer experiments, in *Aspects of Climate Variability in the Pacific and the Western Americas*, *Geophys. Monogr. Ser.*, vol. 55, edited by P. D. H., pp. 237–275, AGU, Washington, D. C.

Hesshaimer, V. (1997), Tracing the global carbon cycle with bomb radiocarbon, Ph.D. thesis, Univ. of Heidelberg, Heidelberg, Germany.

Hesshaimer, V., and I. Levin (2000), Revision of the stratospheric bomb $^{14}CO_2$ inventory, *J. Geophys. Res.*, *105*, 11,641–11,658.

Hesshaimer, V., M. Heimann, and I. Levin (1994), Radiocarbon evidence for a smaller oceanic carbon dioxide sink than previously believed, *Nature*, *370*, 201–203.

Houghton, R. A., and J. L. Hackler (2001), Carbon flux to the atmosphere from land-use changes: 1850 to 1990, *Data Rep. ORNL NDP–050/R1*, Carbon Dioxide Inf. Anal. Cent., Oak Ridge Natl. Lab., Oak Ridge, Tenn.

Jain, A. K., H. S. Kheshgi, and D. J. Wuebbles (1997), Is there an imbalance in the global budget of bomb-produced radiocarbon?, *J. Geophys. Res.*, *102*, 1327–1333.

Johnston, H. S. (1989), Evaluation of excess carbon 14 and strontium 90 data for suitability to test two-dimensional stratospheric models, *J. Geophys. Res.*, *94*, 18,485–18,493.

Johnston, H. S., D. Kattenhorn, and G. Whitten (1976), Use of excess carbon 14 data to calibrate models of stratospheric ozone depletion and supersonic transports, *J. Geophys. Res.*, *81*, 368–380.

Joos, F. (1994), Imbalance in the budget, *Nature*, *370*, 181–182.

Keeling, C. D., and T. P. Whorf (2004), Atmospheric CO_2 records from sites in the SIO air sampling network, in *Trends: A Compendium of Data on Global Change*, Carbon Dioxide Inf. Anal. Cent., Oak Ridge Natl. Lab., Oak Ridge, Tenn.

Keeling, C. D., R. B. Bacastow, A. F. Carter, S. C. Piper, T. P. Whorf, M. Heimann, W. G. Mook, and H. Roeloffzen (1989), A three-dimensional model of atmospheric CO_2 transport based on observed winds, 1. Analysis of observational data, in *Aspects of Climate Variability in the Pacific and the Western Americas*, *Geophys. Monogr. Ser.*, vol. 55, edited by D. H. Peterson, pp. 165–236, AGU, Washington, D. C.

Key, R. M., A. Kozyr, C. L. Sabine, K. Lee, R. Wanninkhof, J. L. Bullister, R. A. Feely, F. J. Millero, C. Mordy, and T.-H. Peng (2004), A global ocean carbon climatology: Results from Global Data Analysis Project (GLODAP), *Global Biogeochem. Cycles*, *18*, GB4031, doi:10.1029/2004GB002247.

Kjellström, E., J. Feichter, and G. Hoffmann (2000), Transport of SF_6 and $^{14}CO_2$ in the atmospheric general circulation model ECHAM4, *Tellus, Ser. B*, *52*, 1–18.

Land, C., J. Feichter, and R. Sausen (2002), Impact of vertical resolution on the transport of passive tracers in the ECHAM4 model, *Tellus, Ser. B*, *54*, 344–360.

Lassey, K. R., M. R. Manning, and B. J. O'Brien (1990), An overview of oceanic radiocarbon: Its inventory and dynamics, *CRC Rev. Aquatic Sci.*, *3*, 117–146.

Lassey, K. R., I. Enting, and C. M. Trudinger (1996), The earth's radiocarbon budget: A consistent model of the global carbon and radiocarbon cycles, *Tellus, Ser. B*, *48*, 487–501.

Levin, I., and V. Hesshaimer (2000), Radiocarbon—A unique tracer of global carbon cycle dynamics, *Radiocarbon*, *42*, 69–80.

Levin, I., and B. Kromer (2004), The tropospheric $^{14}CO_2$ level in midlatitudes of the Northern Hemisphere (1959–2003), *Radiocarbon*, *46*, 1261–1272.

Levin, I., B. Kromer, H. Schoch-Fischer, M. Bruns, M. Münnich, D. Berdau, J. C. Vogel, and K. O. Münnich (1985), 25 years of tropospheric ^{14}C observations in Central Europe, *Radiocarbon*, *27*, 1–19.

Levin, I., B. Kromer, D. Wagenbach, and K. O. Münnich (1987), Carbon isotope measurements of atmospheric CO_2 at a coastal station in Antarctica, *Tellus, Ser. B*, *39*, 89–95.

Levin, I., B. Kromer, and R. J. Francey (1999), Continuous measurements of ^{14}C in atmospheric CO_2 at Cape Grim 1995-1996, in *Baseline Atmospheric Program Australia, 1996*, edited by J. L. Grass et al., Bur. of Meteorol. and CSIRO Atmos. Res., Melbourne, Australia.

Lingenfelter, R. E. (1963), Production of carbon 14 by cosmic-ray neutrons, *Rev. Geophys.*, *1*, 35–55.

Maiss, M., L. P. Steele, R. J. Francey, P. J. Fraser, R. L. Langenfelds, N. B. A. Trivett, and I. Levin (1996), Sulfur hexafluoride - a powerful new atmospheric tracer, *Atmos. Environ.*, *30*, 1621–1629.

Manning, M. R., D. C. Lowe, W. H. Melhuish, R. J. Sparks, G. Wallace, C. A. M. Brenninkmeijer, and R. C. McGill (1990), The use of radiocarbon measurements in atmospheric studies, *Radiocarbon*, *32*, 37–58.

Marland, G., T. A. Boden, and R. J. Andres (2003), Global, regional, and national CO_2 emissions, in *Trends: A Compendium of Data on Global Change*, Carbon Dioxide Inf. Anal. Cent., Oak Ridge Natl. Lab., Oak Ridge, Tenn.

Mook, W. G. (2000), Environmental isotopes in the hydrological cycle: Principles and applications, Int. Atom. Energy Agency (IAEA), Vienna, Austria. (Available at http://www.iaea.or.at/programmes/ripc/ih/volumes/volumes.htm)

Mook, W. G., M. Koopmans, A. F. Carter, and C. D. Keeling (1983), Seasonal, latitudinal, and secular variations in the abundance and isotopic ratios of atmospheric carbon dioxide: 1. Results from land stations, *J. Geophys. Res.*, *88*, 10,915–10,933.

Naegler, T. (2005), Simulating bomb radiocarbon: Consequences for the global carbon cycle, Ph.D. thesis, Univ. of Heidelberg, Heidelberg, Germany.

Naegler, T., P. Ciais, K. Rodgers, and I. Levin (2006), Excess radiocarbon constraints on air-sea gas exchange and the uptake of CO_2 by the oceans, *Geophys. Res. Lett.*, doi:10.1029/2005GL025408, in press.

Nakamura, T., T. Nakazawa, N. Nakai, H. Kitagawa, H. Honda, T. Itoh, T. Machida, and E. Matsumoto (1992), Measurement of ^{14}C concentration of stratospheric CO_2 by accelerator mass spectronomy, *Radiocarbon*, *34*, 745–752.

Neftel, A., H. Friedli, E. Moor, H. Lötscher, H. Oeschger, U. Siegenthaler, and B. Stauffer (1994), Historical CO_2 record from the Siple Station ice core, in *Trends: A Compendium of Data on Global Change*, Carbon Dioxide Inf. Anal. Cent., Oak Ridge Natl. Lab., Oak Ridge, Tenn.

Nydal, R., and K. Lövseth (1996), Carbon-14 measurements in atmospheric CO_2 from northern and southern hemisphere sites, 1962-1993, *ORNL/CDIAC-93, NDP-057*, Oak Ridge Natl. Lab., Oak Ridge, Tenn.

Nydal, R., K. Lövseth, and F. A. Skogseth (1980), Transfer of bomb ^{14}C to the ocean surface, *Radiocarbon*, *22*, 626–635.

Oeschger, H., U. Siegenthaler, U. Schotterer, and A. Gugelmann (1975), A box diffusion model to study the carbon dioxide exchange in nature, *Tellus*, *27*, 168–192.

Olson, R. J., M. O. Scurlock, S. D. Prince, D. L. Zheng, and K. R. Johnson (2001), NPP multi-biome: NPP and driver data for ecosystem model, data intercomparison, Oak Ridge Natl. Lab. Dist. Active Arch. Cent., Oak Ridge, Tenn. (Available at http://daac.ornl.gov)

Patra, P. K., S. Lal, B. H. Subbaraya, C. H. Jackman, and P. Rajaratnam (1997), Observed vertical profile of sulphur hexafluoride (SF_6) and its atmospheric applications, *J. Geophys. Res.*, *102*, 8855–8859.

Peacock, S. (2004), Debate over the ocean bomb radiocarbon sink: Closing the gap, *Global Biogeochem. Cycles*, *18*, GB2022, doi:10.1029/2003GB002211.

Post, W. M., III (1993), Organic carbon in soil and the global carbon cycle, in *The Global Carbon Cycle*, *NATO ASI Ser.*, vol. 115, edited by M. Heimann, pp. 277–302, Springer, New York.

Prentice, I. C., et al. (2001), The carbon cycle and atmospheric CO_2, in *Climate Change: The Scientific Basis*, edited by J. T. Houghton et al., pp. 183–237, Cambridge Univ. Press, New York.

Rath, H. (1988), Simulation der globalen ^{85}Kr- und $^{14}CO_2$-Verteilung mit Hilfe eines zeitabhängigen, zweidimensionalen Modells der Atmosphäre, Ph.D. thesis, Univ. Heidelberg, Germany.

Rubin, S., and R. M. Key (2002), Separating natural and bomb-produced radiocarbon in the ocean: The potential alkalinity method, *Global Biogeochem. Cycles*, *16*(4), 1105, doi:10.1029/2001GB001432.

Strunk, M., A. Engel, U. Schmidt, C. M. Volk, T. Wetter, I. Levin, and H. Glatzel-Mattheier (2000), CO_2 and SF_6 as stratospheric age tracers: Consistency of the effect of mesospheric SF_6-loss, *Geophys. Res. Lett.*, *27*, 341–344.

Stuiver, M., P. J. Reimer, J. W. Beck, G. S. Burr, K. A. Hughen, B. Kromer, G. McCormac, J. van der Plicht, and M. Spurk (1998a), INTCAL98 Radiocarbon Age Calibration, 24,000-0 cal BP, *Radiocarbon*, *40*, 1041–1084.

Stuiver, M., P. J. Reimer, and T. F. Braziunas (1998b), High-precision radiocarbon age calibration for terrestrial and marine samples, *Radiocarbon*, *40*, 1127–1151.

Sweeney, C., E. Gloor, A. J. Jacobson, R. M. Key, G. McKinley, and J. Sarmiento (2004), Estimating air-sea gas exchange using bomb ^{14}C: revisited, paper presented at Ocean Sci. Meet., poster, AGU, Portland, Oreg.

Tans, P. (1981), A compilation of bomb ^{14}C data for use in global carbon cycle model calculations, in *SCOPE 16, Carbon Cycle Modelling*, edited by B. Bolin, pp. 131–137, John Wiley, Hoboken, N. J.

Telegadas, K. (1971), The seasonal atmospheric distribution and inventories of excess carbon-14 from March 1955 to July 1969, *HASL Rep. 243*, Health and Safety Lab., U.S. Atmos. Energy Comm., New York.

Telegadas, K., and R. J. List (1969), Are particulate radioactive tracers indicative of stratospheric motions?, *J. Geophys. Res.*, *74*, 1339–1350.

U.N. Science Committee on the Effects of Atomic Radiation (UNSCEAR) (1993), Sources and effects of ionizing radiation, in *UNSCEAR 1993 Report to the General Assembly*, *Tech. Pap.*, Vienna. (Available at http://www.unscear.org/)

UNSCEAR (2000), Sources and effects of ionizing radiation, in *UNSCEAR 2000 Report to the General Assembly*, *Tech. Pap.*, U.N. Sci. Comm. on the Effects of Atom. Radiation, Vienna. (Available at http://www.unscear.org/)

Wagenbach, D. (1996), Coastal Antarctica: Atmospheric chemical composition and atmospheric transport, in *Chemical Exchange Between the Atmosphere and Polar Snow*, *NATO ASI Workshop*, edited by E. Wolf and R. Bales, pp. 173–199, Springer, New York.

Wanninkhof, R. (1992), Relationship between wind speed and gas exchange over the ocean, *J. Geophys. Res.*, *97*, 7373–7382.

Yang, X., R. North, and C. Romney (2000), CMR nuclear explosion database (revision 3), *CMR Tech. Rep. 00/16*, Cent. for Monitor. Res., U. S. Army Space and Missile Defense Command, Arlington, Va.

I. Levin and T. Naegler, Institut für Umweltphysik, INF 229, D-69120 Heidelberg, Germany. (tobias.naegler@iup.uni-heidelberg.de)